

Original Article

Open Access



Expression of ALKBH3 and its effects on proliferation, migration, and invasion of lung adenocarcinoma A549 cells: bioinformatics analysis and *in vitro* and *in vivo* experiments

Song Zhang, Haoyu Chen, Tao Liu, Chao Qin, Hang Yan, Haiyang Hu, Shengjie Tang, Tingting Dai, Danyu Ji, Li Yang, Haining Zhou

Based Laboratory Center of Suining City Hospital Affiliated to Chongqing Medical University, Chongqing Medical University Affiliated Suining City Central Hospital Thoracic Surgery, Suining 629000, Sichuan, China.

Correspondence to: Dr. Li Yang, Based Laboratory Center of Suining City Hospital Affiliated to Chongqing Medical University, Chongqing Medical University Affiliated Suining City Central Hospital Thoracic Surgery, 127 Desheng West Road, Chuanshan District, Suining 629000, Sichuan, China. E-mail: liyang159357258@126.com; Dr. Haining Zhou, Based Laboratory Center of Suining City Hospital Affiliated to Chongqing Medical University, Chongqing Medical University Affiliated Suining City Central Hospital Thoracic Surgery, 127 Desheng West Road, Chuanshan District, Suining 629000, Sichuan, China. E-mail: haining_zhou@zmu.edu.cn

How to cite this article: Zhang S, Chen H, Liu T, Qin C, Yan H, Hu H, Tang S, Dai T, Ji D, Yang L, Zhou H. Expression of ALKBH3 and its effects on proliferation, migration, and invasion of lung adenocarcinoma A549 cells: bioinformatics analysis and *in vitro* and *in vivo* experiments. *J Cancer Metastasis Treat* 2024;10:32. <https://dx.doi.org/10.20517/2394-4722.2024.109>

Received: 17 Oct 2024 **First Decision:** 26 Nov 2024 **Revised:** 10 Dec 2024 **Accepted:** 19 Dec 2024 **Published:** 31 Dec 2024

Academic Editor: Ciro Isidoro **Copy Editor:** Fangling Lan **Production Editor:** Fangling Lan

Abstract

Objective: To use bioinformatics analysis and *in vitro* and *in vivo* experiments to study the biological role of ALKBH3 in lung adenocarcinoma.

Methods: Bioinformatics analysis of ALKBH3 was performed using databases. ALKBH3 expression in lung adenocarcinoma and adjacent tissues was detected by qPCR (quantitative polymerase chain reaction), western blotting, and immunohistochemistry. Stable transformed A549 cells with low expression of ALKBH3 were constructed. The effects of knockdown of ALKBH3 on the proliferation, migration, and invasion of lung adenocarcinoma A549 cells were detected by CCK-8, cell scratch, and transwell invasion assays, respectively. The effects of ALKBH3 on the proliferation of A549 cells *in vivo* were detected using subcutaneous tumorigenesis in nude mice.



© The Author(s) 2024. **Open Access** This article is licensed under a Creative Commons Attribution 4.0 International License (<https://creativecommons.org/licenses/by/4.0/>), which permits unrestricted use, sharing, adaptation, distribution and reproduction in any medium or format, for any purpose, even commercially, as long as you give appropriate credit to the original author(s) and the source, provide a link to the Creative Commons license, and indicate if changes were made.



Results: Bioinformatics analysis showed that ALKBH3 has diagnostic value in tumors such as lung adenocarcinoma, the expression of ALKBH3 is related to immune cell infiltration, ALKBH3 interacts with ASCC family molecules, and ALKBH3 is involved in the demethylation of DNA and RNA. The expression of ALKBH3 in lung adenocarcinoma was higher than that in adjacent tissues ($P < 0.05$). CCK-8, wound healing and transwell assays showed that ALKBH3 knockdown significantly inhibited the proliferation, migration, and invasion of A549 cells *in vitro* ($P < 0.01$). ALKBH3 knockdown also significantly inhibited the growth of subcutaneous tumors in nude mice ($P < 0.01$).

Conclusions: ALKBH3 is a potential diagnostic marker for lung adenocarcinoma. Results *in vivo* and *in vitro* showed that knocking down ALKBH3 could inhibit the proliferation, migration, invasion, and subcutaneous tumorigenesis of lung adenocarcinoma A549 cells.

Keywords: ALKBH3, lung adenocarcinoma, cell proliferation, cell migration, cell invasion

INTRODUCTION

Among all malignant tumors, lung cancer, particularly lung adenocarcinoma, has the highest mortality and morbidity rates^[1]. There are a variety of treatments available for lung cancer, including surgery, chemotherapy, radiotherapy, molecular targeted therapy, and immunotherapy. In patients with advanced lung cancer, the overall treatment effect is still unsatisfactory, resulting in a 5-year survival rate of less than 20% due to tumor proliferation and distant metastasis^[2,3]. In this regard, there is a need to elucidate more fully the molecular mechanisms underlying lung cancer proliferation and metastasis in order to develop new treatment strategies.

Epigenetic dysregulation, a common feature of human cancers, promotes tumorigenesis and the maintenance of malignant phenotypes by regulating gene expression^[4]. Epigenetic modification includes the chemical modification of DNA, proteins, and RNA. RNA epigenetic modification is the regulation mode at the post-transcriptional level^[5,6]. As the most common and important pair of epigenetic modifications, methylation and demethylation regulate tumorigenesis, tumor development, migration, and invasion of tumor cells, which have attracted people's attention^[7-9]. Alpha-ketoglutarate-dependent dioxygenase homolog 3 (ALKBH3) is a recently discovered novel M6A demethylase belonging to the ALKB family. It has important roles in protecting cells from DNA damage and regulating gene expression and protein translation^[10-13], as well as in maintaining genomic stability and regulating RNA transcription, and its abnormal expression and function have been implicated in the occurrence of many cancers^[13,14]. Lu *et al.* found that enhancing the stability of ALKBH3 mRNA could promote proliferation and invasion of hepatocellular carcinoma cells^[15]. In addition, Woo and Chambers found that overexpression of ALKBH3 increased the invasion of ovarian and breast cancer cells^[16]. ALKBH3 has also been shown to accelerate the survival, angiogenesis, and invasion of urothelial carcinomas^[17]. Tasaki *et al.* found that ALKBH3 significantly contributes to lung adenocarcinoma cancer cell survival through *in vivo* experiments^[18]. Although previous studies have elucidated some functions and implications of ALKBH3 in cancer cells, the role and significance of ALKBH3 in lung adenocarcinoma cells *in vitro* remain largely unexplored. Furthermore, the function and significance of ALKBH3 in lung adenocarcinoma cells were further validated through the transplantation of tumor cells at various sites in nude mice.

We began by analyzing ALKBH3 expression in lung adenocarcinoma and pan-cancer tissues to determine its effects on biological behaviors. Furthermore, we investigated the relationship between ALKBH3 expression and immune infiltration, as well as genetic changes and epigenetic status. The study utilized lung adenocarcinoma tissue, normal lung tissue, a lung adenocarcinoma tissue microarray, the lung

adenocarcinoma A549 cell line, and nude mice. First, ALKBH3 expression was assessed using western blotting, real-time quantitative polymerase chain reaction (RT-qPCR), and immunohistochemistry (IHC). Next, a stable transformed cell line consisting of lung adenocarcinoma A549 cells with low ALKBH3 expression was constructed. Through CCK-8 assays *in vitro*, transwell and cell scratch assays, and subcutaneous tumorigenesis experiments in nude mice, we found ALKBH3 could inhibit lung adenocarcinoma A549 cell proliferation, migration, and invasion.

MATERIALS AND METHODS

Bioinformatics analysis

ALKBH3 expression levels

Differences in gene expression were analyzed using the Assistant for Clinical Bioinformatics website (<https://www.aclbi.com/static/index.html#/tcga>), based on data from The Cancer Genome Atlas (TCGA) and the Genotype-Tissue Expression project (GTEx). We obtained a lung adenocarcinoma dataset ($n = 516$) and normal tissue samples (TCGA, 59 cases; GTEx, 578 cases). Differential gene expression between the two samples was analyzed using the Wilcoxon rank sum test. Level 3 RNA sequencing data from TCGA and GTEx version 8 were used (<https://gtexportal.org/home/datasets>), and calculations were performed in R version 4.0.3 to identify statistically significant differences. In addition, we used R to analyze the expression of ALKBH3 in pan-cancer tissues based on TCGA data.

ALKBH3 expression and immune cell infiltration

TIMER2.0 (<http://timer.cistrome.org/>) is an online database that provides comprehensive data on the immune cells that are infiltrating tumors. In this study, we used the “Immune” and “Exploration” modules in TIMER2.0 to analyze the correlations between ALKBH3 expression levels and immune cell infiltration levels, EGFR expression levels, and mutation status in lung adenocarcinoma.

Based on expression data, the European Prospective Investigation into Cancer and Nutrition (EPIC)^[19] (https://gfellerlab.shinyapps.io/EPIC_1-1/) provides infiltration ratios for eight types of immune cells. We calculated stromal, immune, and ESTIMATE scores based on TCGA data; then, we used EPIC to evaluate the relationships between ALKBH3 and immune cells on a pan-cancer basis.

Protein-protein interaction network analysis

GeneMANIA, an online database for protein-protein interaction networks developed by the University of Toronto^[20-22], was used to explore the protein molecules that interact and are co-expressed with ALKBH3 in lung adenocarcinoma and to predict the functions of target genes.

Mutations and epigenetic alterations

The cBioPortal enables the analysis and interpretation of cancer genetic data and facilitates the interpretation of molecular data obtained from cancer histological and cytological studies^[23] (<http://www.cbioportal.org>). Genetic data from 2,922 samples of 2,583 pan-cancer patients were analyzed using the UCSC Xena and the International Cancer Genome Union’s “TCGA Pan-Cancer Map Research” data portal.

ALKBH3 promoter DNA methylation levels in normal and pan-cancer tissues were examined using UALCAN (<http://ualcan.path.uab.edu/analysis.html>)^[24]. DNA methylation levels are represented by beta values, indicating hypomethylation (beta: 0.3-0.25) or hypermethylation (beta: 0.7-0.5)^[25].

Tissue experiments in lung adenocarcinoma

Clinical sample

Patients at Suining Central Hospital in 2023 who had not received any antineoplastic therapy (including radiotherapy, chemotherapy, targeted therapy, and immunotherapy) were enrolled, and 16 pairs of fresh lung adenocarcinoma tissues and adjacent tissues (further than 3 cm from the tumor margin) were collected. ALKBH3 protein and mRNA expression levels were measured by western blotting and RT-qPCR. The Ethics Committee of Suining Central Hospital approved this study (approval number: KYLLKS20230109). A lung adenocarcinoma tissue chip (array number: HLugA180Su11; chip batch number: XT21-011) was used for IHC.

Real-time quantitative PCR

To isolate total RNA from tissues, TRIzol reagent was used. We used a reverse transcription kit to reverse transcribe RNA into cDNA and performed RT-qPCR according to the instructions provided with the RT-qPCR kit (Shenzhen Apuno Biomedical Technology Co., Ltd.). To calculate relative mRNA expression levels, GAPDH was used as a control gene. The primers used were as follows: GAPDH, GAAAGCCTGCCGGTGACTAA (positive) and TCACGTCAACAAAGCCAGGA (reverse); ALKBH3, AGCCACGAGTGATTGACAGA (positive) and TCACGTCAACAAAGCCAGGA (reverse).

Western blotting analysis

Frozen tissue samples were cracked with a strong PIPA cleavage solution and crushed with a homogenizer. Using the BCA method, the protein concentration was determined after low-temperature ultracentrifugation. In this study, proteins were separated by 10% sodium dodecyl sulfate-polyacrylamide gel electrophoresis and transferred to polyvinylidene fluoride membranes (PVDF). After sealing with 5% skimmed milk powder, according to the instructions provided with the antibodies against ALKBH3 and β -actin, diluted with antibody diluent, the membranes were incubated overnight in a refrigerator at 4 °C. Target gene bands and internal reference gene bands of the same variety were cultured in a greenhouse for 1 h. Then, the ECL developer was dropped evenly on the PVDF membranes, and they were exposed to a gel chemiluminescence imager. For each lane, the gray value ratio was calculated using ImageJ software.

IHC analysis

The IHC staining experiments were carried out by RocheVentanaBenchMark at the Department of Pathology, Suining Central Hospital. The degree of positivity was determined based on the extent of color development: colorless, 0; light yellow, 1; light brown, 2; dark brown, 3. The scoring system was as follows: 5%, 0 points; 6%-25%, 1 point; 26%-50%, 2 points; 51%-75%, 3 points; > 75%, 4 points. For the product of the two fractions, 0-6 was considered to indicate low expression and > 6 to denote high expression.

Experiments with lung adenocarcinoma cell line A549

Cell line, culture, and transfection

A549 cells are one of the types of human lung adenocarcinoma cells. Due to their easy culture, clear genetic background, and stability, A549 cells have been widely used in cancer biology, gene function and toxicology studies, especially those related to lung adenocarcinoma. Therefore, A549 cells were selected for experiments in this study. Lung adenocarcinoma A549 cells were purchased from Wuhan Irrette Biotechnology Co., Ltd., cultured in RPMI1640 medium supplemented with fetal bovine serum and 1% penicillin-streptomycin, and preserved at 37 °C under 5% carbon dioxide. The lentiviruses used in this experiment were constructed and packaged by Shanghai Jikai Basic Technology Co., Ltd. Three different lentiviruses were used: Lv-ALKBH3-RNAi-1, Lv-ALKBH3-RNAi-2, and Lv-ALKBH3-RNAi-3. The lentivirus negative control was LVCON303 (hu6-mts-cbh-gcgfp-ires-purromycin). The experimental group was divided into a blank control group (culture of normal A549 cells), an empty vector control group (A549

cells transfected with negative control), knockdown group 1 (LV-ALKBH3-RNAi-1 transfection), knockdown group 2 (LV-ALKBH3-RNAi-2 transfection), and knockdown group 3 (LV-ALKBH3-RNAi-3 transfection).

A 1 mL cell suspension and 1 mL of culture medium were added to a 6-well plate, designating one well as the blank control group, which received only culture medium. Another well served as the negative control group, receiving empty carrier lentivirus, while the remaining well was assigned to the infected virus group, treated with ALKBH3 knockdown lentivirus. Following 72 h of infection, the cell fusion rate under the microscope reached approximately 80%, prompting immediate screening of the infected cells. The cells were subsequently cultured in the puromycin-containing medium at a concentration of 2 $\mu\text{g}/\text{mL}$. After 24 h of culture, all cells in the blank control group perished, whereas the remaining cells in the negative control and infected groups survived, resulting in a stable A549 cell line with ALKBH3 knockdown. Western blotting and real-time quantitative PCR were employed to assess the TPM4 knockout efficiency.

Cell proliferation test (CCK-8 assay)

The stable transformants of ALKBH3 knockdown group 1 (LV-ALKBH3-RNAi-1) and knockdown group 2 (LV-ALKBH3-RNAi-2) were detected by CCK-8 assay. For each group, three accessory wells were set up, and 100 μL phosphate-buffered saline (PBS) solution was added to the remaining well. After the cells adhered to the walls of the wells, fresh medium (100 mL) and CCK-8 reagent (10 mL) were added, and the plate was incubated at 37 $^{\circ}\text{C}$, 5% CO_2 . The absorbance values of each hole were measured and recorded at 450 nm using an enzyme labeling instrument. The experiment was repeated three times, and a proliferation curve was constructed based on the results.

Cell scratch assay

A cell suspension of A549 cells with low ALKBH3 expression was diluted to a concentration of 5×10^5 cells/mL and inoculated into six-well plates with three accessory holes for each group; then, 1 mL culture medium was added to each well. When the cells had reached confluence within each well, a 100 μL pipette tip was used to create a scratch from one end of the well to the other. Images were obtained under a microscope (Thermo Fisher Scientific, USA) at 0, 24, and 48 h. Results were analyzed, compared, and plotted based on three repeats of the experiment.

Transwell invasion assay

Cell invasion was investigated using a transwell assay. The matrigel matrix was diluted with serum-free medium at a 1:8 ratio at 4 $^{\circ}\text{C}$. Then, 60 μL of the diluted Matrigel matrix was dropped onto the polycarbonate film of each transwell chamber, and the apparatus was placed in a Matrigel incubator at 37 $^{\circ}\text{C}$ overnight. Cells with a 90% confluence and good growth conditions were trypsinized, centrifuged, and the supernatant discarded. The cells were resuspended in 2 mL PBS solution and washed twice. A 100 μL aliquot of the cell suspension, containing 5×10^5 cells/mL, was added to each Transwell chamber. Transwell plates were then filled with 600 μL of 20% fetal bovine serum medium. After 24 h of incubation, the cells in the upper chamber were gently wiped off with a cotton swab. The cells were fixed for 15 min by the addition of 4% paraformaldehyde (600 μL) to the 24-well plate, air-dried at room temperature and then stained with 600 μL crystal violet solution. Infected cells were observed using an inverted microscope (Thermo Fisher Scientific, USA). For each group, three randomly selected visual fields were imaged and counted. The experiment was repeated three times. After image processing, data were collected for analysis, and a statistical histogram was constructed.

Subcutaneous tumorigenesis in nude mice

Logarithmic-phase A549 cells and A549 cells exhibiting low-level ALKBH3 expression were harvested and adjusted to a concentration of 1×10^7 cells/mL. Male nude mice, aged 6 to 8 weeks and procured from Guangzhou Kexun Biotechnology Co., LTD., were selected, excluding those with physical frailty, underlying diseases, or behavioral abnormalities. The mice were randomly assigned into three groups: the control group ($n = 10$), knockout group 1 ($n = 10$), and knockout group 2 ($n = 10$). Prior to subcutaneous injection, the injection site of the nude mice was disinfected with 75% ethanol. The cell suspension was gently agitated to ensure homogeneity, preventing aggregation and optimizing cell viability. Each mouse received a subcutaneous injection of 200 μ L of cell suspension, containing 2×10^6 cells, into the anterior axillary region, chosen for its abundant blood supply. The growth of the mice was monitored continuously. Once subcutaneous tumors formed, the body weight and tumor volume of each mouse were recorded daily. Mice were euthanized upon the tumor reaching a volume of 1.5×10^3 mm³. The tumors were excised, weighed, and photographed against a white background using vernier calipers, facilitating the construction of a statistical analysis of tumor weight.

Statistical analysis

The statistical methods employed in the bioinformatics analysis are comprehensively described in the “Experimental Methods” section of this study. Continuous variable data are presented as Mean \pm Standard Error of the Mean (Mean \pm SEM). Tests for normality and homogeneity of variance were conducted to compare the means of two independent samples. When both assumptions were satisfied, a two-sample *t*-test was applied. In cases where homogeneity of variance was not satisfied, an approximate *t*-test or Mann-Whitney U test was used. One-way Analysis of Variance (ANOVA) was conducted for pairwise comparisons among multiple groups. For comparisons of two sample proportions, the χ^2 test or Fisher’s exact test was applied. The significance threshold for all statistical analyses in this study was set at $\alpha = 0.05$. Statistical significance was denoted as follows: * for $P < 0.05$, ** for $P < 0.01$, *** for $P < 0.001$, and **** for $P < 0.0001$. A $P > 0.05$ indicated no statistical significance. Data storage, analysis, visualization, and graphical representation were performed using Excel, IBM SPSS 26.0, GraphPad Prism 9.5.1, ImageJ, and Adobe Illustrator 2022.

RESULTS

Bioinformatics analysis

TPM4 expression levels

First, we used the Clinical Bioinformatics Assistant website to analyze the gene expression differences of ALKBH3 in cancers including lung adenocarcinoma. For differential gene expression analysis, 516 tumor samples and 637 normal samples were obtained (59 paracancerous tissue samples from TCGA and 578 normal tissue samples from GTEx). The expression levels of ALKBH3 in the two groups of samples were analyzed using the R software package ggplot2. In lung adenocarcinoma tissues, ALKBH3 expression was significantly higher than in adjacent tissues [Figure 1A]. ALKBH3 levels were significantly elevated in CHOL (cholangiocarcinoma), COAD (Colon adenocarcinoma), GBM (Glioblastoma multiforme), HNSC (Head and Neck squamous cell carcinoma), KIRC (Kidney renal clear cell carcinoma), LIHC (Liver hepatocellular carcinoma), LUSC (Lung squamous cell carcinoma), PCPG (Pheochromocytoma and Paraganglioma), and PRAD (Prostate adenocarcinoma) based on the TCGA and GTEx datasets. By contrast, ALKBH3 was downregulated in BRCA and UCEC [Figure 1B].

Protein-protein interaction network analysis

Online databases were used to explore protein molecules that interact and co-express with ALKBH3 in lung adenocarcinoma and predict the functions of target genes. As shown in Figure 1C, we observed interactions

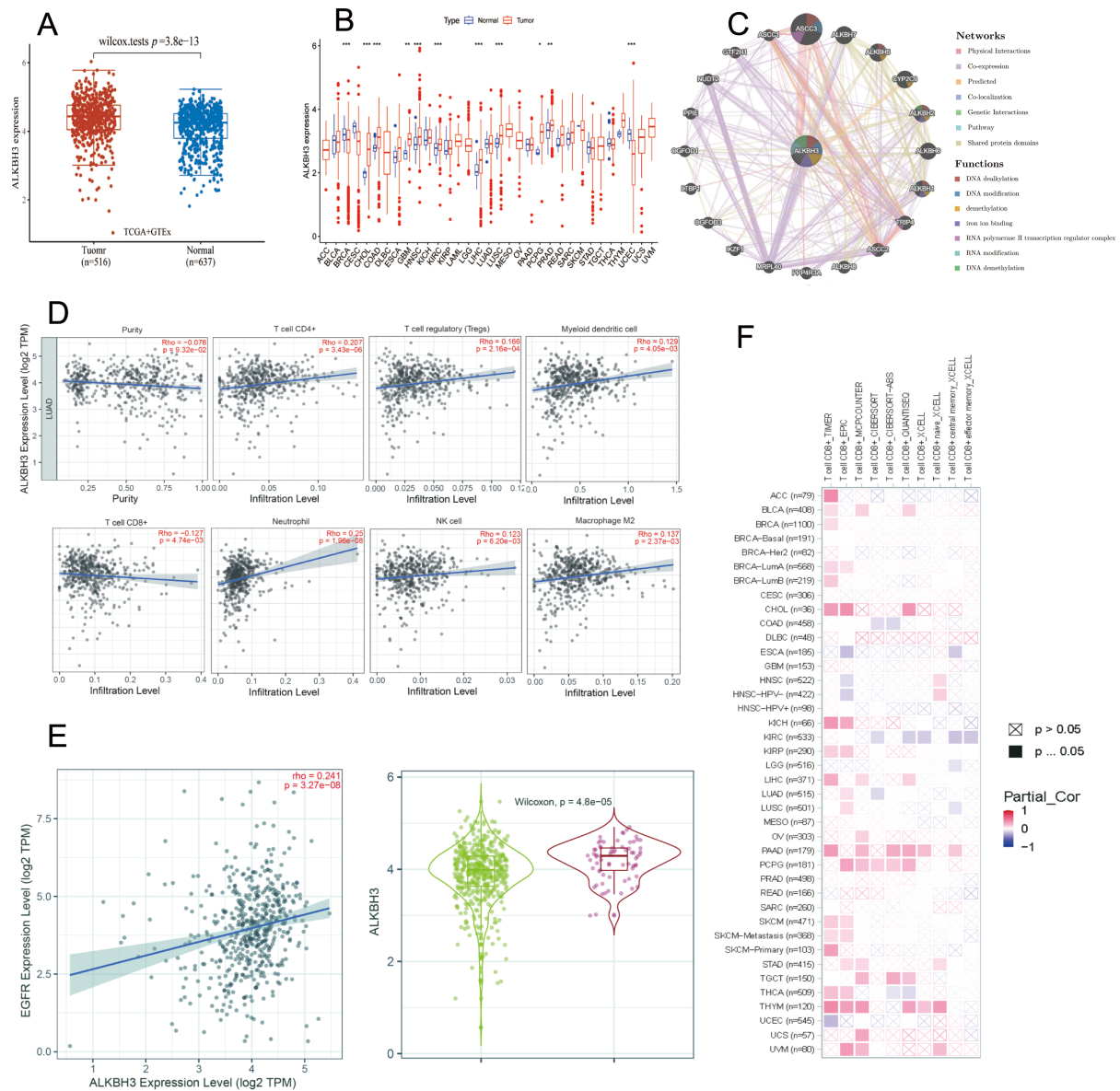


Figure 1. ALKBH3 expression and immune cell infiltration. (A) Expression levels of ALKBH3 in adjacent tissues and tumor tissues based on Assistant for Clinical Bioinformatics ($n = 1,153$). (B) The expression of ALKBH3 in pan-cancer tissues based on TCGA data ($*P < 0.05$; $**P < 0.01$; $***P < 0.001$). (C) Protein-Protein interaction networks with ALKBH3 as the target gene. (D) Correlation analysis between the expression level of ALKBH3 and the level of immune cell infiltration in LUAD (TIMER2.0). (E) Correlation analysis of ALKBH3 with the expression level and mutation status of *EGFR* (TIMER2.0). (F) ALKBH3 expression and immune cell infiltration.

of ALKBH3 with ASCC3, ASCC2, and ASCC in lung adenocarcinoma, especially ASCC3. There was also a co-expression relationship between ALKBH3 and ALKBH2. Gene function prediction showed that the interaction between ALKBH3 and ASCC3 might be involved in the metabolism of DNA. ALKBH3 is involved in the demethylation of DNA and RNA, as well as in important biological processes such as iron-iron binding [Figure 1C].

ALKBH3 expression and immune cell infiltration

Secondly, the online database and statistical software were used to analyze the correlation between ALKBH3 expression level and immune cell infiltration level, EGFR expression level, and mutation status in lung adenocarcinoma tissue. CD4⁺ and regulatory T cells, bone marrow dendritic cells, neutrophils, natural killer cells, and macrophages were positively correlated with the expression of ALKBH3 in lung adenocarcinomas. Infiltration levels of M2 macrophages were positively correlated with those of CD8⁺ T cells [Figure 1D]. Moreover, we found a positive correlation between ALKBH3 and EGFR expression in lung adenocarcinomas. Compared with wild-type EGFR, mutant EGFR lung adenocarcinoma had higher expression levels of ALKBH3, and the difference was statistically significant [Figure 1E].

Our study used the EPIC online tool to determine if ALKBH3 expression is associated with immune cell infiltration within the tumor microenvironment. Eight types of cancer-associated immune cells were linked to ALKBH3 expression in various cancers, notably PAAD, PCPG, and THYM [Figure 1F].

Mutations and epigenetic alterations

Next, we used online databases to analyze mutations and epigenetic alterations in ALKBH3. Our investigation of pan-cancer genetic alterations within ALKBH3 was conducted using cBioPortal. ALKBH3 expression was altered in 2.0% of 51 samples collected from 2,565 cancer patients. ALKBH3 mutation was observed in 28 cancers, with bladder cancer showing the highest ALKBH3 mutation rate. Lung cancer is characterized by amplification-type copy number variations [Figure 2A and B].

In addition to assessing methylation levels in the promoter DNA of ALKBH3, we examined 20 types of cancer tissues. Hypermethylation was found in BRCA, CHOL, COAD, and other tumor types [Figure 2C].

ALKBH3 protein is highly expressed in lung adenocarcinoma

In this section, we used WB and immunohistochemistry to detect the expression level of ALKBH3 protein in lung adenocarcinoma tissues and adjacent tissues. Tissue microarray detection of 80 samples of lung adenocarcinoma and 88 samples of paraneoplastic tissues showed that positive expression of ALKBH3 was mainly located in the cytoplasm. Tissue microarray analysis showed that ALKBH3 expression was high in 38 of the 80 lung adenocarcinoma samples (IHC score > 6) and low in 42 samples (IHC score ≤ 6). In the 88 paraneoplastic tissue samples, the expression of ALKBH3 was high in one (1.14%) and low in 87 cases (98.86%). In lung adenocarcinoma, ALKBH3 expression was significantly higher than in adjacent tissues ($P < 0.001$; Figure 3, Table 1). The relative expression of ALKBH3 protein in 12 pairs of fresh lung adenocarcinoma and matched paraneoplastic tissues was detected by western blotting. The expression levels of ALKBH3 in lung adenocarcinoma were significantly higher than those in paraneoplastic tissues ($P < 0.0001$; Figure 4A and B). Lung adenocarcinomas express high levels of the ALKBH3 protein.

ALKBH3 is highly expressed in lung adenocarcinoma

To further explore the expression of ALKBH3 in lung adenocarcinoma, we carried out RT-qPCR experiments. The relative expression of ALKBH3 mRNA in four pairs of fresh lung adenocarcinoma and matched paraneoplastic tissues was detected. In lung adenocarcinoma, ALKBH3 mRNA expression was significantly higher compared to paraneoplastic tissue based on the results of cDNA amplification ($P < 0.05$, Figure 4C).

Effects of ALKBH3 on proliferation, migration, and invasion of A549 cells

Effect of ALKBH3 expression on proliferation of A549 cells

First of all, we detected overexpression of ALKBH3 in lung adenocarcinoma by RT-qPCR and western blotting experiments. To further study the significance of ALKBH3 expression in lung adenocarcinoma, we

Table 1. ALKBH3 protein expression levels in LUAD and paracancerous tissues

Group	High expression	Low expression	$\chi \rightarrow P$
CT [n (%)]	38 (47.50)	42 (52.50)	47.97 < 0.001
ANT [n (%)]	1 (1.14)	87 (98.86)	

constructed a stable mutant strain of A549 cells with low ALKBH3 expression via knockdown of ALKBH3. Western blotting and RT-qPCR showed that this stable transmutation had been successfully constructed [Figure 4D-F]. Then, we used a CCK-8 assay to evaluate the effects of ALKBH3 on A549 cells. The proliferation rates of ALKBH3 stable mutant cells in knockout group 1 and knockout group 2 were significantly lower than that of normal A549 cells ($P < 0.05$, Figure 4G). Thus, our experimental data show that knocking down ALKBH3 can inhibit the proliferation of A549 cells.

Effects of ALKBH3 expression on migration and invasion of A549 cells

Next, we tested the migration and invasion of A549 cells using a transwell assay and a scratch assay. The results of the cell scratch test showed that the healing ability of the ALKBH3-knockout A549 cell line was significantly weaker than that of the control group at 72 h ($P < 0.01$, Figure 5A and B). Moreover, the transwell assay showed that A549 cells with low ALKBH3 expression were significantly less invasive than the control group ($P < 0.01$, Figure 5C and D). In summary, our results indicate that knocking down ALKBH3 can reduce invasiveness.

Knockdown of ALKBH3 can inhibit the growth of subcutaneous tumors in nude mice

At last, we subcutaneously injected stable A549 cells and normal A549 cells with low ALKBH3 levels into nude mice to further verify the role of ALKBH3 *in vivo*. When subcutaneous tumors began to form, the mouse body weights and subcutaneous tumor volumes were recorded every day. When the subcutaneous tumors grew to more than $1.5 \times 10^3 \text{ mm}^3$, the nude mice were dissected, and the tumor growth was observed. As can be seen from Figure 5E, the subcutaneous tumor volumes of ALKBH3 knockdown group 1 and ALKBH3 knockdown group 2 were significantly smaller than those of the normal group ($P < 0.001$, Figure 5E and F). Overall, these results indicate that ALKBH3 knockdown prevents lung adenocarcinoma growth.

DISCUSSION

Adenocarcinoma accounts for about 40% of non-small-cell lung cancers, and lung cancer has the highest morbidity and mortality rates of all cancers worldwide^[26,27]. Therefore, it is of great significance to explore new diagnosis and treatment targets for lung adenocarcinoma.

Firstly, we investigated the expression of ALKBH3 and its effects on lung adenocarcinoma's biological behavior and function. By analyzing publicly available data, we found that ALKBH3 was highly expressed in lung adenocarcinomas. The expression of ALKBH3 was also upregulated in some cancer tissues, according to pan-cancer analysis. These results suggest that ALKBH3 has potential applications as a marker for some tumor types. Human immunotherapy has led to the development of new treatment strategies for cancer patients and has greatly changed the pattern of oncology. As a result of the heterogeneity of the tumor microenvironment, not all patients benefit from immunotherapy or maintain a long-term clinical response. ALKBH3 expression levels were positively correlated with CD4⁺ T cells, regulatory T cells, myeloid dendritic cells, neutrophils, natural killer cells, and M2 macrophage infiltration levels in lung adenocarcinoma, but negatively correlated with CD4⁺ T cells. These results suggest that ALKBH3 could affect the sensitivity of patients to immunotherapy and could also be used as a therapeutic target. Notably,

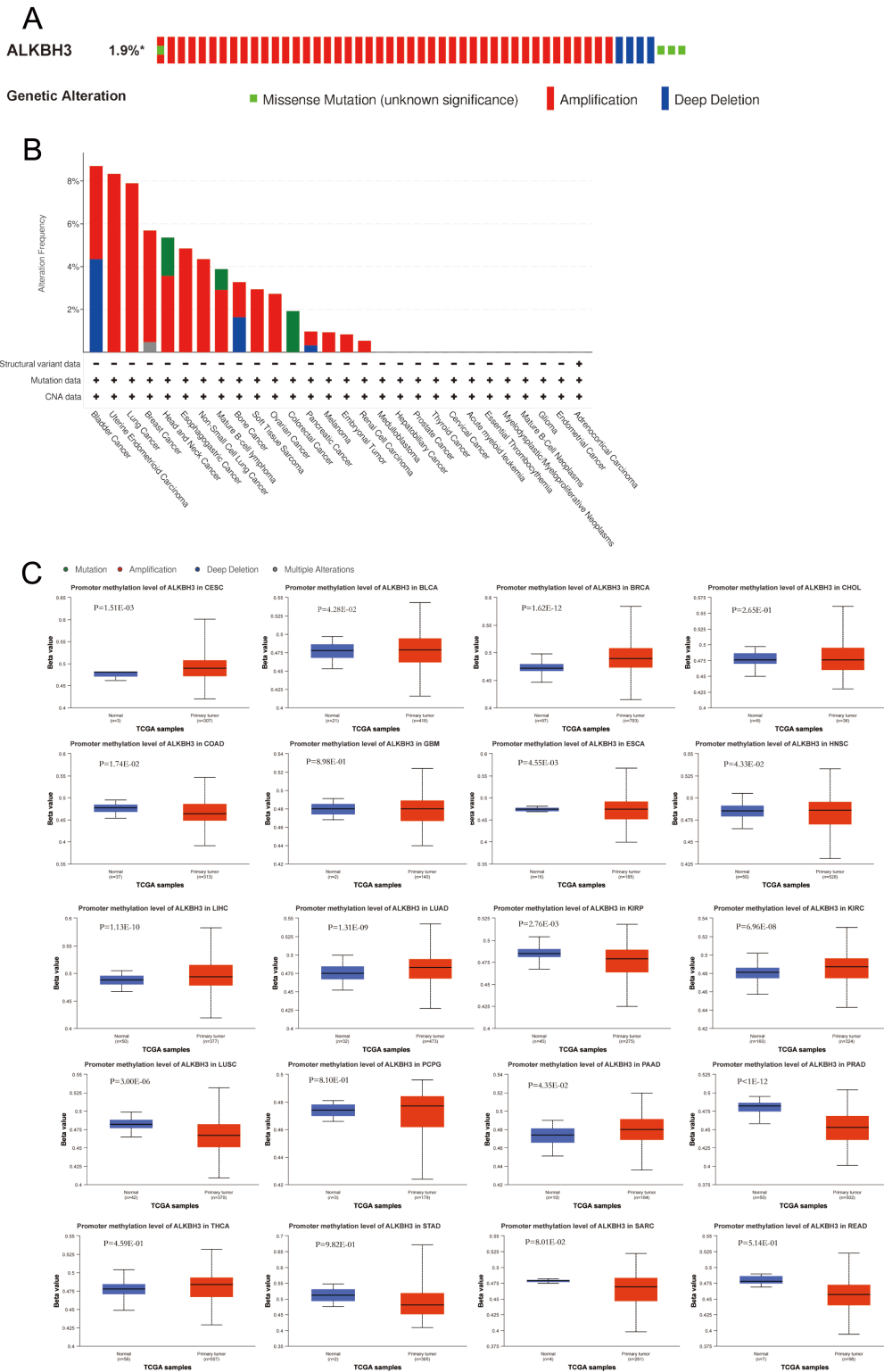


Figure 2. Genetic alteration analysis and promoter methylation level in ALKBH3. (A) Genetic alteration in ALKBH3 in pan-cancer tissues, accounting for 5% of alterations. (B) The alteration frequency with the mutation type of ALKBH3 in different cancers. (C) Promoter methylation level in ALKBH3 between adjacent tissues and tumor tissues in 20 types of cancer from UALCAN.

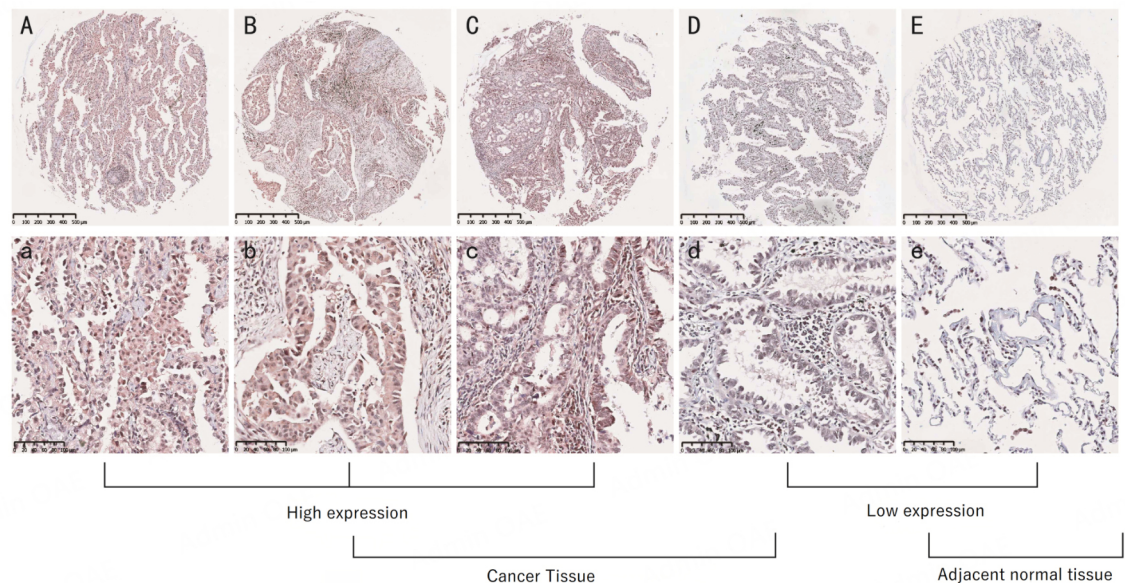


Figure 3. Relative expression levels of ALKBH3 in lung adenocarcinoma and paracarcinoma tissues (IHC staining, with a scale bar included in the image).

ALKBH5, another family member, has been shown to modulate anti-PD-1 therapy response by influencing lactate levels in the tumor microenvironment and altering immune cell infiltration, indicating a potential overlapping role in immune modulation^[28]. Gene function prediction results showed that the interaction between ALKBH3 and ASCC3 may be involved in the metabolic process of DNA. ALKBH3 is involved in the demethylation of DNA and RNA and is also related to important biological processes such as iron-iron binding. In addition, mutations and epigenetic changes can lead to abnormal gene expression. We found that ALKBH3 had a high mutation frequency in lung cancer. Moreover, we assessed the levels of ALKBH3 promoter DNA methylation in 19 cancer tissues and found that ALKBH3 was hypermethylated in BRCA, CHOL, COAD, and other tumors. Previous studies have shown that the AlkB family can catalyze demethylation on a variety of substrates (such as RNA and DNA), thereby affecting tumor progression and prognosis^[29-31]. *In vitro*, western blotting, RT-qPCR, and IHC techniques were used to further verify that the expression of ALKBH3 in lung adenocarcinoma was significantly upregulated. This is consistent with previous studies that found that ALKBH3 is differentially expressed in various cancer types, such as pancreatic cancer, prostate cancer, and renal cancer^[32-34]. To further explore the effects of ALKBH3 on the biological behavior and function of lung adenocarcinoma, A549 cells and nude mice were used to construct a stable lung adenocarcinoma cell line with ALKBH3 knockout. CCK-8 assay *in vitro*, transwell assay, cell scratch assay, and subcutaneous tumor formation in nude mice were used to assess the effects of ALKBH3 on the proliferation, migration, and invasion of A549 cells. Compared to cells in the blank control group and empty vector group, A549 cells with low ALKBH3 expression exhibited significantly reduced proliferation, migration, and invasion. The oncogenic role of ALKBH3 in tumor growth is likely attributed to its regulation of mRNA stability and translation of genes that govern cell proliferation, which occurs through the activation of the PI3K/AKT and MAPK/ERK signaling pathways, thus facilitating tumor progression. Furthermore, its involvement in mitigating RNA damage and sustaining cancer cell survival under stress conditions further consolidates its pro-tumorigenic function. *In vivo* and *in vitro* experiments on subcutaneous tumor formation in nude mice showed that knockdown of ALKBH3 inhibited the growth of subcutaneous tumors. In addition, the role of ALKBH3 in cellular invasion and migration is likely attributed to its enhancement of the invasion and migratory capabilities of cancer cells, primarily through the modulation of epithelial-mesenchymal transition (EMT). This process involves the upregulation of

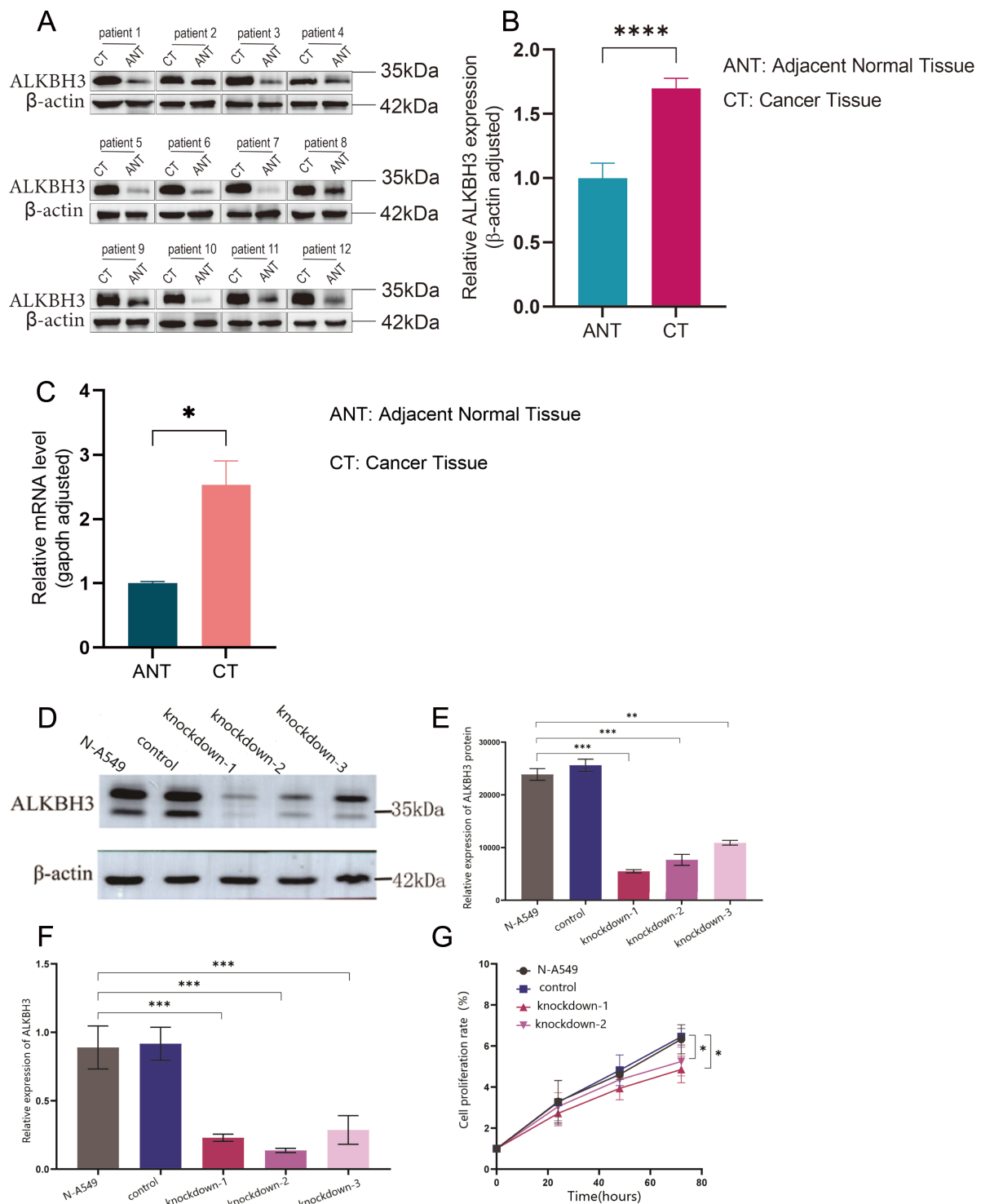


Figure 4. Expression of ALKBH3. (A) Detection of ALKBH3 protein levels in 12 pairs of fresh LUAD and paracarcinomas using Western blot. (B) Statistical analyses and bar graphs of the relative expression of *ALKBH3* protein in 12 pairs of LUAD and paracarcinomas. (**** indicates $P < 0.0001$). (C) Relative expression of *ALKBH3* mRNA in 4 pairs of fresh LUAD and paired paracarcinomas detected by RT-qPCR (* indicates $P < 0.05$). (D) Strip graph. (E and F) Statistical graph. (G) Proliferation curve. (* indicates $P < 0.05$, *** indicates $P < 0.001$).

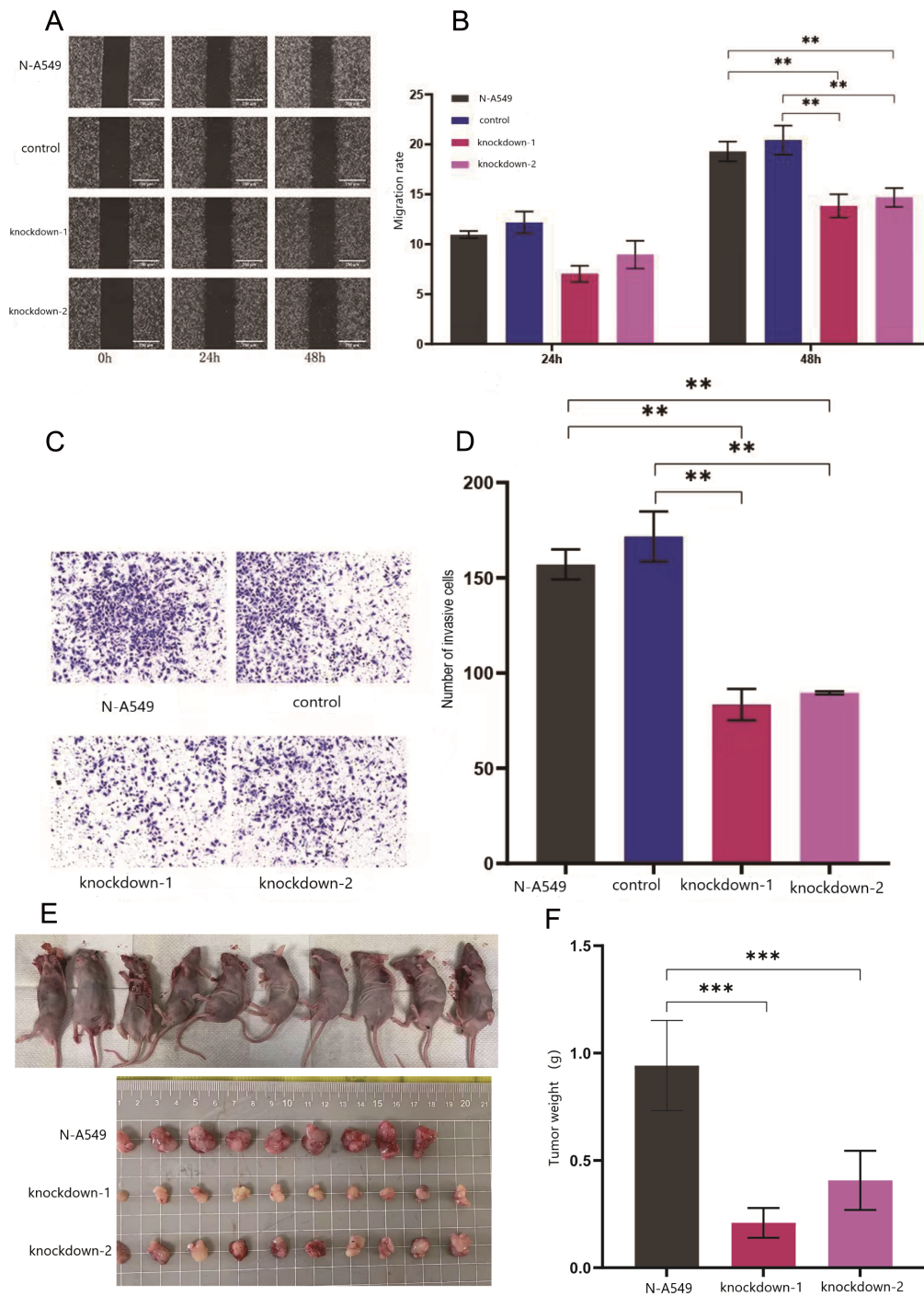


Figure 5. Effects of ALKBH3 expression on migration and invasion of A549 cells. (A) the healing of four groups of cells. (B) Statistical diagram of cell migration rate of the four groups (** indicates $P < 0.01$). (C) Invasion ability of four groups of cells. (D) Statistical chart of the number of invasive cells in four groups of cells (** indicates $P < 0.01$). (E) Nude mice and subcutaneous tumors of nude mice. (F) Statistical graph of subcutaneous tumor weights of three groups (***) indicates $P < 0.001$).

EMT-related transcription factors and matrix metalloproteinases (MMPs), degradation of the extracellular matrix (ECM) barrier, and subsequent promotion of metastatic dissemination. The results of this study further confirmed the findings of Tasaki *et al.*^[18]. In addition, these results are consistent with previous

studies showing that ALKBH3 is involved in the progression of some cancers, such as prostate cancer, salivary gland tumors, and liver cancer, suggesting that inhibiting ALKBH3 may provide a viable therapeutic approach^[32,35,36]. According to the above experimental results, ALKBH3 is a potential diagnostic biomarker and therapeutic target for lung adenocarcinoma.

Overall, our results support the role of ALKBH3 as an oncogene in the growth, invasion, and migration of lung adenocarcinoma cells. These findings will further our understanding of the tumor microenvironment in lung adenocarcinoma and provide valuable data for further exploration of its pathogenesis and potential therapeutic targets. However, this study has some limitations. Although A549 cells are of great value in the study of lung adenocarcinoma, they still have limitations. This study can be verified in other cell lines or patient-derived organoids to more fully reveal the biological mechanism and therapeutic potential of lung adenocarcinoma. Cell cycle and apoptosis assays can also be used to fully explore the role of ALKBH3 in lung adenocarcinoma cell function. Additionally, while we have established a link between ALKBH3 expression and immune cell infiltration, the exact mechanisms underlying this relationship require further exploration.

This study highlights ALKBH3 as a promising diagnostic biomarker for Lung adenocarcinoma, with its elevated expression serving as an indicator of aggressive disease. Therapeutically, targeting ALKBH3 could curb tumor proliferation and metastasis, either through small molecule inhibitors or RNA-based approaches. Additionally, its connection to immune cell infiltration suggests it could influence immune evasion, paving the way for combination therapies with immune checkpoint inhibitors. Building upon these findings, future investigations should focus on: elucidating the molecular mechanisms linking ALKBH3 to immune cell infiltration, with a particular focus on its role in shaping the tumor microenvironment; investigating the potential of ALKBH3 inhibitors in preclinical models, particularly their efficacy in halting the progression of lung adenocarcinoma and enhancing response to current therapeutic strategies; exploring ALKBH3's role in other RNA modifications and their downstream effects, which could provide valuable insights into the broader implications of RNA epigenetics in the pathogenesis of lung adenocarcinoma; and conducting clinical studies to validate ALKBH3 as a biomarker for patient stratification and prognostic prediction, potentially improving personalized treatment approaches. Therefore, further studies and clinical trials are necessary to confirm the clinical value of ALKBH3 as a clinical diagnostic and prognostic indicator, paving the way for improved clinical outcomes in lung adenocarcinoma management.

DECLARATIONS

Acknowledgments

We acknowledge the use of TCGA, GTEx, TIMER2.0, EPIC, GeneMANIA, cBioPortal, and UALCAN free of cost.

Authors' contribution

Conceptualization: Zhang S, Zhou H, Chen H, Liu T

Methodology, formal analysis, visualization, and writing original draft: Zhang S, Chen H, Liu T, Tang S

Software: Hu H, Liu T, Qin C, Dai T, Yan H, Tang S

Experiment validation: Zhang S, Qin C, Chen H, Yan H, Liu T

Data collection: Qin C, Yan H, Dai T, Yang L, Ji D

Project administration and funding acquisition: Zhou H, Yang L, Zhang S

All authors contributed to the article and approved the submitted version.

Availability of data and materials

The datasets generated and/or analyzed during the current study are available from the corresponding author upon reasonable request.

Financial support and sponsorship

This study was funded by the Sichuan Provincial Health Commission Project Fund (No. 21PJ188).

Conflicts of interest

All authors declared that there are no conflicts of interest.

Ethical approval and consent to participate

The study was conducted in accordance with the principles of the Declaration of Helsinki. It was approved by the Medical Research Ethics Review Committee of Suining Central Hospital. The ethical approval code is: KYLLKS20240054. All participants provided written informed consent prior to their inclusion in the study.

Consent for publication

Not applicable.

Copyright

© The Author(s) 2024

REFERENCES

1. Herbst RS, Morgensztern D, Boshoff C. The biology and management of non-small cell lung cancer. *Nature* 2018;553:446-54. [DOI PubMed](#)
2. Allemani C, Matsuda T, Di Carlo V, et al. Global surveillance of trends in cancer survival 2000-14 (CONCORD-3): analysis of individual records for 37 513 025 patients diagnosed with one of 18 cancers from 322 population-based registries in 71 countries. *Lancet* 2018;391:1023-75. [DOI](#)
3. Oudkerk M, Liu S, Heuvelmans MA, Walter JE, Field JK. Lung cancer LDCT screening and mortality reduction - evidence, pitfalls and future perspectives. *Nat Rev Clin Oncol* 2021;18:135-51. [DOI PubMed](#)
4. Zhu Z, Qian Q, Zhao X, Ma L, Chen P. N⁶-methyladenosine ALKBH5 promotes non-small cell lung cancer progress by regulating TIMP3 stability. *Gene* 2020;731:144348. [DOI](#)
5. Yang P, Wang Q, Liu A, Zhu J, Feng J. ALKBH5 holds prognostic values and inhibits the metastasis of colon cancer. *Pathol Oncol Res* 2020;26:1615-23. [DOI](#)
6. Zhang J, Guo S, Piao HY, et al. ALKBH5 promotes invasion and metastasis of gastric cancer by decreasing methylation of the lncRNA NEAT1. *J Physiol Biochem* 2019;75:379-89. [DOI PubMed PMC](#)
7. Roundtree IA, Evans ME, Pan T, He C. Dynamic RNA modifications in gene expression regulation. *Cell* 2017;169:1187-200. [DOI PubMed PMC](#)
8. Xu J, Liu Y, Liu J, et al. The identification of critical m⁶A RNA methylation regulators as malignant prognosis factors in prostate adenocarcinoma. *Front Genet* 2020;11:602485. [DOI PubMed PMC](#)
9. Fu Y, Dominissini D, Rechavi G, He C. Gene expression regulation mediated through reversible m⁶A RNA methylation. *Nat Rev Genet* 2014;15:293-306. [DOI PubMed](#)
10. Tang C, Klukovich R, Peng H, et al. ALKBH5-dependent m⁶A demethylation controls splicing and stability of long 3'-UTR mRNAs in male germ cells. *Proc Natl Acad Sci USA* 2018;115:E325-33. [DOI PubMed PMC](#)
11. Zou S, Toh JDW, Wong KHO, Gao YG, Hong W, Woon ECY. N⁶-methyladenosine: a conformational marker that regulates the substrate specificity of human demethylases FTO and ALKBH5. *Sci Rep* 2016;6:25677. [DOI PubMed PMC](#)
12. Huang H, Weng H, Chen J. m⁶A modification in coding and non-coding RNAs: roles and therapeutic implications in cancer. *Cancer Cell* 2020;37:270-88. [DOI PubMed PMC](#)
13. Ueda Y, Ooshio I, Fusamae Y, et al. AlkB homolog 3-mediated tRNA demethylation promotes protein synthesis in cancer cells. *Sci Rep* 2017;7:42271. [DOI PubMed PMC](#)
14. Jiang X, Liu B, Nie Z, et al. The role of m6A modification in the biological functions and diseases. *Signal Transduct Target Ther* 2021;6:74. [DOI PubMed PMC](#)
15. Lu Q, Wang H, Lei X, et al. lncRNA ALKBH3-AS1 enhances ALKBH3 mRNA stability to promote hepatocellular carcinoma cell proliferation and invasion. *J Cell Mol Med* 2022;26:5292-302. [DOI PubMed PMC](#)

16. Woo HH, Chambers SK. Human ALKBH3-induced m¹A demethylation increases the CSF-1 mRNA stability in breast and ovarian cancer cells. *Biochim Biophys Acta Gene Regul Mech* 2019;1862:35-46. DOI PubMed
17. Shimada K, Fujii T, Tsujikawa K, Anai S, Fujimoto K, Konishi N. ALKBH3 contributes to survival and angiogenesis of human urothelial carcinoma cells through NADPH oxidase and tweak/Fn14/VEGF signals. *Clin Cancer Res* 2012;18:5247-55. DOI PubMed
18. Tasaki M, Shimada K, Kimura H, Tsujikawa K, Konishi N. ALKBH3, a human AlkB homologue, contributes to cell survival in human non-small-cell lung cancer. *Br J Cancer* 2011;104:700-6. DOI PubMed PMC
19. Yeo JG, Wasser M, Kumar P, et al. The extended polydimensional immunome characterization (EPIC) web-based reference and discovery tool for cytometry data. *Nat Biotechnol* 2020;38:679-84. DOI
20. Warde-Farley D, Donaldson SL, Comes O, et al. The GeneMANIA prediction server: biological network integration for gene prioritization and predicting gene function. *Nucleic Acids Res* 2010;38:W214-20. DOI PubMed PMC
21. Zuberi K, Franz M, Rodriguez H, et al. GeneMANIA prediction server 2013 update. *Nucleic Acids Res* 2013;41:W115-22. DOI PubMed PMC
22. Franz M, Rodriguez H, Lopes C, et al. GeneMANIA update 2018. *Nucleic Acids Res* 2018;46:W60-4. DOI PubMed PMC
23. Cerami E, Gao J, Dogrusoz U, et al. The cBio cancer genomics portal: an open platform for exploring multidimensional cancer genomics data. *Cancer Discov* 2012;2:401-4. DOI PubMed PMC
24. Chandrashekar DS, Bashel B, Balasubramanya SAH, et al. UALCAN: a portal for facilitating tumor subgroup gene expression and survival analyses. *Neoplasia* 2017;19:649-58. DOI PubMed PMC
25. Men C, Chai H, Song X, Li Y, Du H, Ren Q. Identification of DNA methylation associated gene signatures in endometrial cancer via integrated analysis of DNA methylation and gene expression systematically. *J Gynecol Oncol* 2017;28:e83. DOI PubMed PMC
26. Sung H, Ferlay J, Siegel RL, et al. Global cancer statistics 2020: GLOBOCAN estimates of incidence and mortality worldwide for 36 cancers in 185 countries. *CA Cancer J Clin* 2021;71:209-49. DOI
27. Xu JY, Zhang C, Wang X, et al. Integrative proteomic characterization of human lung adenocarcinoma. *Cell* 2020;182:245-61.e17. DOI
28. Li N, Kang Y, Wang L, et al. ALKBH5 regulates anti-PD-1 therapy response by modulating lactate and suppressive immune cell accumulation in tumor microenvironment. *Proc Natl Acad Sci USA* 2020;117:20159-70. DOI PubMed PMC
29. Bian K, Lenz SAP, Tang Q, et al. DNA repair enzymes ALKBH2, ALKBH3, and AlkB oxidize 5-methylcytosine to 5-hydroxymethylcytosine, 5-formylcytosine and 5-carboxylcytosine in vitro. *Nucleic Acids Res* 2019;47:5522-9. DOI PubMed PMC
30. Wu TP, Wang T, Seetin MG, et al. DNA methylation on N⁶-adenine in mammalian embryonic stem cells. *Nature* 2016;532:329-33. DOI PubMed PMC
31. Wu G, Yan Y, Cai Y, et al. ALKBH1-8 and FTO: potential therapeutic targets and prognostic biomarkers in lung adenocarcinoma pathogenesis. *Front Cell Dev Biol* 2021;9:633927. DOI PubMed PMC
32. Koike K, Ueda Y, Hase H, et al. Anti-tumor effect of AlkB homolog 3 knockdown in hormone- independent prostate cancer cells. *Curr Cancer Drug Targets* 2012;12:847-56. DOI
33. Yamato I, Sho M, Shimada K, et al. PCA-1/ALKBH3 contributes to pancreatic cancer by supporting apoptotic resistance and angiogenesis. *Cancer Res* 2012;72:4829-39. DOI
34. Hotta K, Sho M, Fujimoto K, et al. Clinical significance and therapeutic potential of prostate cancer antigen-1/ALKBH3 in human renal cell carcinoma. *Oncol Rep* 2015;34:648-54. DOI
35. Marcinkowski M, Garbicz D, Pilżys T, Kukwa W, Grzesiuk E. Selected ALKBH dioxygenases are overexpressed in salivary gland tumours. *Acta Biochim Pol* 2022;69:889-94. DOI PubMed
36. Wang Q, Wang G, Wang Y, Liu C, He X. Association of AlkB homolog 3 expression with tumor recurrence and unfavorable prognosis in hepatocellular carcinoma. *J Gastroenterol Hepatol* 2018;33:1617-25. DOI